Gas-Phase Reactions of Atomic Lanthanide Cations with CO_2 and CS_2: Room-Temperature Kinetics and Periodicities in Reactivity

Ping Cheng, Gregory K. Koyanagi, and Diethard K. Bohme*

Department of Chemistry, Centre for Research in Mass Spectrometry and Centre for Research in Earth and Space Science, York University, Toronto, Ontario, Canada M3J 1P3

Received: June 15, 2006; In Final Form: September 21, 2006

Gas-phase reactions of atomic lanthanide cations (excluding Pm^+) have been surveyed systematically with CO_2 and CS_2 using an inductively coupled plasma/selected-ion flow tube (ICP/SIFT) tandem mass spectrometer. Observations are reported for reactions with La^+, Ce^+, Pr^+, Nd^+, Sm^+, Eu^+, Gd^+, Tb^+, Dy^+, Ho^+, Er^+, Tm^+, Yb^+, and Lu^+ at room temperature (295 ± 2 K) in helium at a total pressure of 0.35 ± 0.02 Torr. The observed primary reaction channels correspond to X-atom transfer (X = O, S) and CX_2 addition. X-atom transfer is the predominant reaction channel with La^+, Ce^+, Pr^+, Nd^+, Gd^+, Tb^+, and Lu^+, and CX_2 addition occurs with the other lanthanide cations. Competition between these two channels is seen only in the reactions of CS_2 with Nd^+ and Lu^+. Rate coefficient measurements indicate a periodicity in the reaction efficiencies of the early and late lanthanides. With CO_2 the observed trends in reactivity across the row and with exothermicity follow trends in the energy required to achieve two unpaired non-f valence electrons by electron promotion within the Ln^+ cation that suggest the presence of a kinetic barrier, in a manner much like those observed previously for reactions with isoelectronic N_2O. In contrast, no such barrier is evident for S-atom transfer from the valence isolectronic CS_2 molecule which proceeds at unit efficiency, and this is attributed to the much higher polarizability of CS_2 compared to CO_2 and N_2O. Up to five CX_2 molecules were observed to add sequentially to selected Ln^+ and LnX^+ cations.

1. Introduction

The recent experimental activity in measurements of gas-phase reactions of atomic lanthanide cations with small molecules has provided new fertile ground for the exploration of fundamental aspects of chemical reactivity.[1−5] Gas-phase reactivities of isolated lanthanide cations began to be studied in the late 1980s with Fourier transform mass spectrometry and various ion-beam techniques, together with laser ablation techniques to produce the atomic cations.[1,6,7] Numerous investigations over the past 20 years have made available extensive data on the gas-phase reactions of the lanthanide cations with various inorganic and organic molecules including hydrogen,[8] oxygen and nitrous oxide,[9] D_2O,[10] alkanes and cycloalkanes,[1,3,7] alkenes,[1,6,11] alcohols,[2,4,12] benzene and substituted benzenes,[13,14] phenol,[15] orthoformates,[13,16] ferrocene and Fe pentacarbonyl,[17] methyl fluoride,[18] and methyl chloride.[5] Generally, these studies show that the reactivity of Ln^+ varies along the 4f series in terms of both the ionic products formed and the reaction efficiencies. These variations have been related to the accessibility of excited electron configurations with two unpaired non-f electrons, that is, to the energies required to excite the ground states of the Ln^+ cations, typically from $4f^n5d^06s^1$ to the $4f^{n-1}5d^16s^1$ states. A recent bonding configuration analysis by Gibson[19] suggests that two unpaired 5d valence electrons rather than a 5d and a 6s electron enable efficient bonding between the metal center and the oxygen atom in LnO^+. The variations in the promotion energies required to achieve either $5d^2$ or $5d^16s^1$ excitation are qualitatively similar across the Ln^+ family and result in similar predictions for the periodic and Arrhenius-like dependencies of the efficiencies of O-atom transfer on the electron promotion energy, except for differences in characteristic temperature. Here we add experimental observations of reactions of atomic lanthanide cations with CO_2 and the related CS_2 molecule to the database.

Surprisingly, to the best of our knowledge, there are no previous reports on the reactions of lanthanide cations with either carbon dioxide or carbon disulfide, although reactions of other metal cations with these two gases now have been surveyed by several groups,[20−23] including our own.[24,25] CO_2 and CS_2 are interesting reagent gases to compare in terms of their chemical activities since they are valence isoelectronic. Furthermore, CO_2 is isoelectronic with N_2O, for which we have previously reported an experimental study of lanthanide ion chemistry.[9] Measurements of the temperature dependence of rate coefficients for gas-phase reactions of neutral lanthanide atoms with CO_2 recently reported by Campell also are available for comparison.[26] Large variations in reactivity were observed, and the reaction energy barrier was found to correlate with the energy required to promote an electron out of the filled 6s subshell. Here we shall explore the influence of electron promotion energy on the reactivities of atomic lanthanide cations at room temperature.

2. Experimental Method

The experimental results reported here were obtained with the inductively coupled plasma/selected-ion flow tube (ICP/SIFT) tandem mass spectrometer that has been described in detail previously.[9,27,28] The atomic ions were generated within atmospheric-pressure argon plasma at 5500 K fed with a vaporized solution containing the lanthanide salt. Solutions containing the metal salt of interest having a concentration of

* Corresponding author. Phone: (416) 736-2100, ext 66188. Fax: (416) 736-5936. E-mail: dkbohme@yorku.ca.

10.1021/jp0637431 CCC: $33.50
Published on Web 11/04/2006

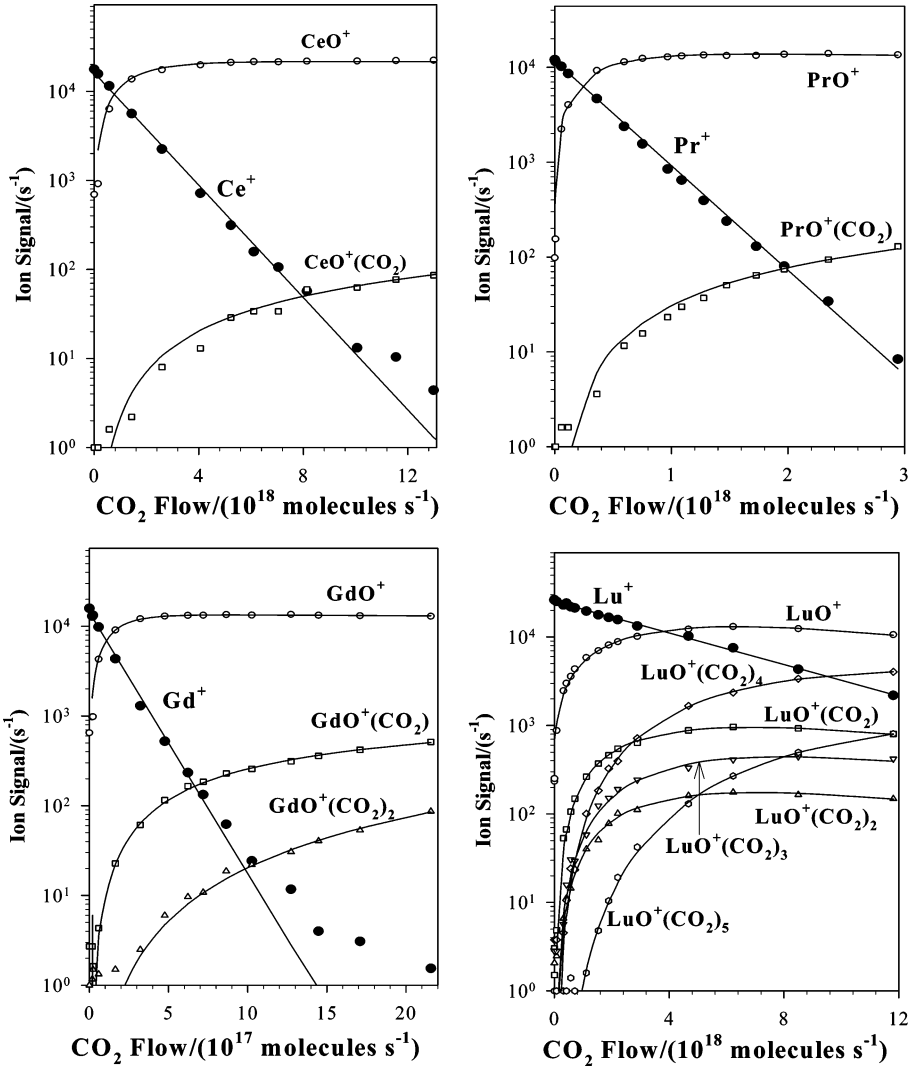

Figure 1. Composite of ICP/SIFT results for reactions of lanthanide metal cations Ce^+, Pr^+, Gd^+, and Lu^+ with CO_2 in helium buffer gas at 0.35 ± 0.01 Torr and 295 ± 2 K.

ca. 5 μg L^{-1} were peristaltically pumped via a nebulizer into the plasma. The plasma gas flow was adjusted to maximize the ion signal detected downstream of the SIFT. The sample solutions were prepared using atomic spectroscopy standard solutions commercially available from SPEX, Teknolab, J. T. Baker Chemical Co., Fisher Scientific Company, Perkin-Elmer, and Alfa Products. The ions emerging from the ICP were injected through a differentially pumped sampling interface into a quadrupole mass filter and, after mass analysis, introduced through an aspirator-like interface into flowing helium carrier gas at 0.35 ± 0.01 Torr and 295 ± 2 K. After experiencing about 10^5 collisions with He atoms, the ions were allowed to react with CO_2 or CS_2 added into the flow tube.

The lanthanide ions emerging from the plasma initially have a Boltzmann internal energy distribution characteristic of the plasma temperature. However, these emerging populations are expected to relax during the approximately 20 ms duration before entry into the reaction region in the flow tube. Energy degradation can occur by radiative decay as well as by collisions with argon atoms and the 10^5 collisions with He before entry into the reaction region. Electronic states of the lanthanides, due to the presence of f electrons, are a mixture of states with both positive and negative parity. This means that there are a large number of parity allowed transitions that will occur quickly ($\sim 10^{-8}$ s), changing their original state distribution from the ICP. La^+ itself is an exception for lanthanides in that it behaves like a transition-metal ion since it does not have any low-lying states with occupied f orbitals. The extent to which quenching of any electronically excited states of the lanthanide cations that may be formed within the ICP is complete is uncertain and could be inferred only indirectly from the observed decays of primary ion signals. The observed semilogarithmic decays of the reacting lanthanide cations were invariably linear over a range from two to as much as three decades of ion depletion and so were indicative of single-state populations (or multiple-state populations with equal reactivities). The many collisions with Ar and He between the source and the reaction region should ensure that the atomic ions reach a translational temperature equal to the tube temperature of 295 ± 2 K prior to entering the reaction region.

Reactant and product ions were sampled at the end of the flow tube with a second quadrupole mass filter, and their signals were measured as a function of added reactant. The resulting profiles provide information about reaction rate coefficients and product-ion distributions. Rate coefficients for primary reactions were determined with an uncertainty estimated to be less than ±30% from the semilogarithmic decay of the reactant ion intensity as a function of added reactant.

CS_2 (Matheson Coleman & Bell, ≥99%) was introduced into the reaction region of the SIFT as a dilute mixture of CS_2 vapor

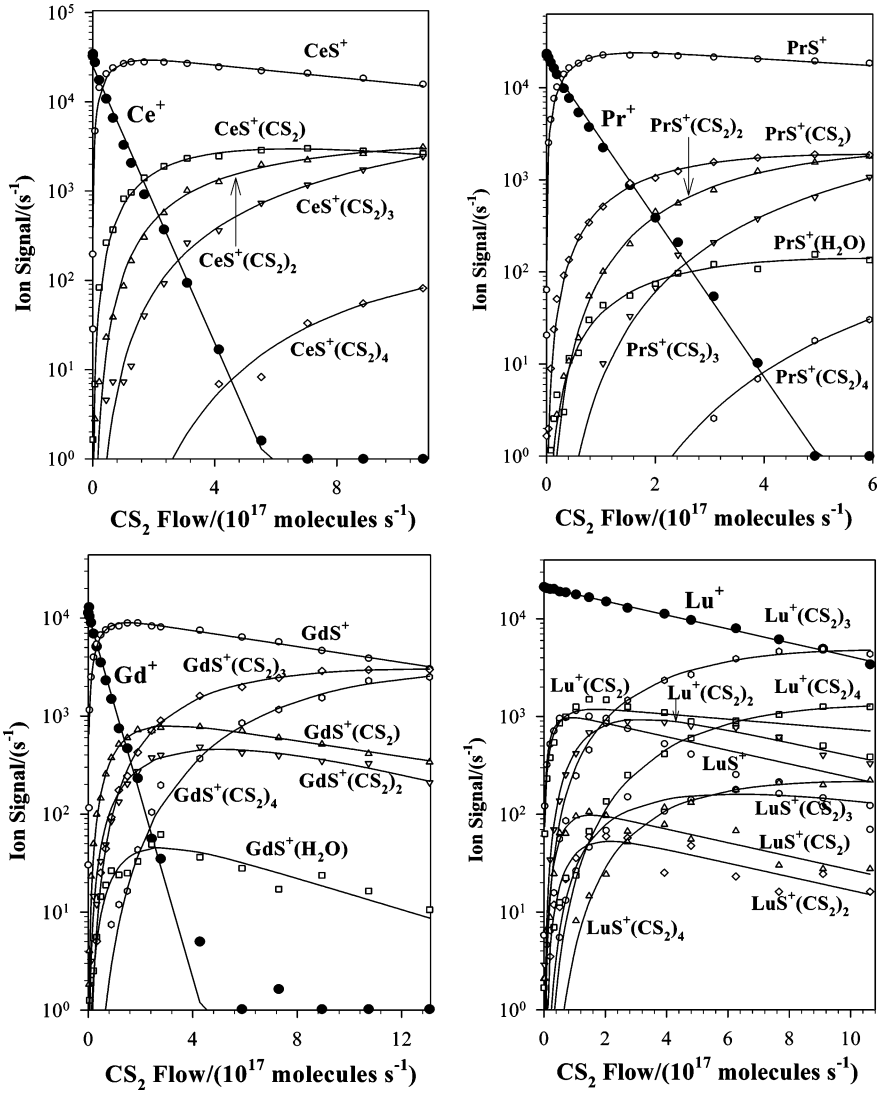

Figure 2. Composite of ICP/SIFT results for reactions of lanthanide metal cations Ce^+, Pr^+, Gd^+, and Lu^+ with CS_2 in helium buffer gas at 0.35 ± 0.01 Torr and 295 ± 2 K.

in helium (~10%), and CO_2 was introduced into the reaction region as a pure gas (Matheson Gas Products, ≥99.9%). The influence of possible impurities in either of these gases can be neglected; all reactions measured to have low efficiencies ($<10^{-2}$ or 10^{-3}) were observed to proceed exclusively by the addition of the added gases.

3. Results and Discussion

The reactions of 14 lanthanide cations were investigated with both CO_2 and CS_2. Both the primary and subsequent chemistries were monitored. Ion profiles obtained for the reactions of Ce^+, Pr^+, Gd^+, and Lu^+ with CO_2 and CS_2 are shown in Figures 1 and 2. Tables 1 and 2 summarize the measured rate coefficients and the derived reaction efficiencies as well as measured product distributions. The reaction efficiency is taken to be equal to the ratio k/k_c, where k is the experimentally measured rate coefficient and k_c is the capture or collision rate coefficient. k_c was computed using the algorithm of the modified variational transition-state/classical trajectory theory developed by Su and Chesnavich[29] with $\alpha(CO_2) = 2.91 \times 10^{-24}$ cm^3 and $\alpha(CS_2) = 8.74 \times 10^{-24}$ cm^3.[30] Figure 3 displays and compares the data in Tables 1 and 2 in a periodic table format.

Only atom transfer, reaction 1a, and adduct formation, reaction 1b, were observed as primary reaction channels (here X may be O or S).

$$Ln^+ + CX_2 \rightarrow LnX^+ + CX \quad (1a)$$

$$Ln^+ + CX_2 \rightarrow Ln^+(CX_2) \quad (1b)$$

As expected from the much lower first ionization energies (IE) of the lanthanides (all values for IE(Ln) < 6.3 eV are much lower than $IE(CO_2) = 13.773 \pm 0.002$ eV and $IE(CS_2) = 10.0685 \pm 0.0020$ eV),[30] electron transfer was not observed with any of the Ln^+ cations.

3.1. Atom Transfer Reactions. O-atom transfer from CO_2 to Ln^+ was observed exclusively with La^+, Ce^+, Pr^+, Nd^+, Gd^+, Tb^+, and Lu^+ with rate coefficients in the range from 3.3×10^{-11} (Lu^+) to 4.6×10^{-10} (Ce^+) cm^3 molecule^{-1} s^{-1}. The efficiencies (k/k_c) for O-atom transfer show a systematic decrease for the first two or three of the early and of the late lanthanides (see Figure 3). S-atom transfer from CS_2 to Ln^+ also was observed exclusively with La^+, Ce^+, Pr^+, Gd^+, and Tb^+, but to compete with CS_2 addition in the reactions of CS_2 with Nd^+ (90%) and Lu^+ (20%). The measured rate coefficients for the exclusive S-atom transfer reactions are all equal to 1.0×10^{-9} cm^3 molecule^{-1} s^{-1}, within experimental uncertainty, and higher than those for the corresponding O-atom transfer

TABLE 1: Rate Coefficients (in Units of 10^{-10} cm^3 molecule^{-1} s^{-1}) and Higher Order Product Ions Measured for Reactions of Atomic Ln^+ Cations with CO_2 in Helium at 0.35 ± 0.01 Torr and 295 ± 2 K[a]

Ln^+	k[b]	k_c	k/k_c	primary products	PD	higher order productions
La^+	4.4	6.91	0.64	LaO^+	100	$LaO^+(CO_2)$
Ce^+	4.6	6.91	0.66	CeO^+	100	$CeO^+(CO_2)$
Pr^+	1.6	6.90	0.23	PrO^+	100	$PrO^+(CO_2)$
Nd^+	0.37	6.89	5.4×10^{-2}	NdO^+	100	$NdO^+(CO_2)_{1-2}$
Sm^+	0.0050	6.83	7.3×10^{-4}	$Sm^+(CO_2)$	100	$Sm^+(CO_2)_{2-3}$
Eu^+	0.0080	6.84	1.2×10^{-3}	$Eu^+(CO_2)$	100	$Eu^+(CO_2)_2$
Gd^+	3.4	6.81	0.50	GdO^+	100	$GdO^+(CO_2)_{1-2}$
Tb^+	0.38	6.81	5.6×10^{-2}	TbO^+	100	$TbO^+(CO_2)_{1-4}$
Dy^+	0.027	6.78	4.0×10^{-3}	$Dy^+(CO_2)$	100	
Ho^+	0.010	6.77	1.5×10^{-3}	$Ho^+(CO_2)$	100	
Er^+	0.0060	6.77	8.9×10^{-4}	$Er^+(CO_2)$	100	
Tm^+	0.0070	6.76	1.0×10^{-3}	$Tm^+(CO_2)$	100	
Yb^+	0.0070	6.75	1.0×10^{-3}	$Yb^+(CO_2)$	100	
Lu^+	0.33	6.73	4.9×10^{-2}	LuO^+	100	$LuO^+(CO_2)_{1-5}$

[a] Products and product distributions (PD in %) are also included along with calculated collision rate coefficients, k_c (in units of 10^{-10} cm^3 molecule^{-1} s^{-1}), and reaction efficiencies, k/k_c (see text). [b] Measured reaction rate coefficient with an estimated accuracy of ±30%.

TABLE 2: Rate Coefficients (in Units of 10^{-10} cm^3 molecule^{-1} s^{-1}) and Higher Order Product Ions Measured for Reactions of Atomic Ln^+ Cations with CS_2 in Helium at 0.35 ± 0.01 Torr and 295 ± 2 K[a]

Ln^+	k[b]	k_c	k/k_c	primary products	PD	higher order product ions
La^+	10	9.87	1.0	LaS^+	100	$LaS^+(CS_2)_{1-3}$
Ce^+	10	9.87	1.0	CeS^+	100	$CeS^+(CS_2)_{1-4}$
Pr^+	10	9.87	1.0	PrS^+	100	$PrS^+(CS_2)_{1-4}$
Nd^+	7.0	9.83	0.71	NdS^+	90	$NdS^+(CS_2)_{1-3}$
				$Nd^+(CS_2)$	10	$Nd^+(CS_2)_{2-4}$
Sm^+	0.74	9.73	7.7×10^{-2}	$Sm^+(CS_2)$	100	$Sm^+(CS_2)_{2-3}$
Eu^+	0.15	9.72	1.6×10^{-2}	$Eu^+(CS_2)$	100	$Eu^+(CS_2)_{2-4}$
Gd^+	9.7	9.68	1.0	GdS^+	100	$GdS^+(CS_2)_{1-4}$
Tb^+	10	9.65	1.0	TbS^+	100	$TbS^+(CS_2)_{1-4}$
Dy^+	0.23	9.62	2.4×10^{-2}	$Dy^+(CS_2)$	100	$Dy^+(CS_2)_{2-4}$
Ho^+	0.29	9.60	3.0×10^{-2}	$Ho^+(CS_2)$	100	$Ho^+(CS_2)_{2-4}$
Er^+	0.44	9.58	4.5×10^{-2}	$Er^+(CS_2)$	100	$Er^+(CS_2)_{2-5}$
Tm^+	0.053	9.56	5.5×10^3	$Tm^+(CS_2)$	100	$Tm^+(CS_2)_{2-3}$
Yb^+	0.060	9.52	6.3×10^{-3}	$Yb^+(CS_2)$	100	$Yb^+(CS_2)_{2-3}$
Lu^+	0.91	9.52	9.6×10^{-2}	LuS^+	20	$LuS^+(CS_2)_{1-4}$
				$Lu^+(CS_2)$	80	$Lu^+(CS_2)_{2-4}$

[a] Products and product distributions (PD in %) are also included along with calculated collision rate coefficients, k_c (in units of 10^{-10} cm^3 molecule^{-1} s^{-1}), and reaction efficiencies, k/k_c (see text). [b] Measured reaction rate coefficient with an estimated accuracy of ±30%.

reactions. Indeed, exclusive S-atom transfer occurs with unit efficiency, within experimental uncertainty.

A second X-atom transfer was not observed with any of the LnX^+ cations.

3.2. Influence of Exothermicity on Atom Transfer. The X-atom affinities of CX are quite high: OA(CO) = 125.75 ± 0.05 kcal mol^{-1} and SA(CS) = 103.8 ± 0.9 kcal mol^{-1}.[31] Thus, X-atom transfer from CX_2 to Ln^+ according to reaction 1a is exothermic and can be expected to occur for those lanthanide cations with a comparable or higher X-atom affinity. The available experimental and theoretical O- and S-atom affinities listed in Table 3 indicate that 11 out of the 14 atomic lanthanide cations have O-atom affinities higher than that of CO, but we observed only seven of these to react measurably with CO_2 by O-atom transfer. The other four cations, Sm^+, Dy^+, Ho^+, and Er^+, all of which have O-atom affinities of ca. 140 kcal mol^{-1}, simply react by CO_2 addition. Figure 4 shows that, with the exception of Lu^+, O-atom transfer actually exhibits an onset at ca. 170 kcal mol^{-1}, viz. at exothermicities larger than ca. 45 kcal mol^{-1}. An analogous onset is apparent in Figure 4 for O-atom transfer from the isoelectronic N_2O molecule for which we have previously reported measured reaction efficiencies,[9] but no such onset is apparent in Figure 4 for the CS_2 reactions that exhibit unit efficiency for exothermic S-atom transfer. The (six) S-atom transfer reactions for which SA(Ln^+) is known generally are less exothermic than the corresponding O-atom transfer reactions, with the exception of Lu^+, with which both O-atom transfer and S-atom transfer are nearly thermoneutral. Apparently a kinetic barrier that decreases with increasing exothermicity operates for O-atom transfer from CO_2 and N_2O, but not for S-atom transfer from CS_2.

3.3. Role of Electron Promotion. We know from our previous studies of O-atom transfer from N_2O to Ln^+ that electron promotion is required (for most Ln^+ cations) to make available two non-f valence electrons for covalent bonding with O in the formation of the oxide cation LnO^+ (the orbitals of f electrons cannot extend far enough spatially to become involved in bonding). A similar requirement is expected for reactions of Ln^+ with the isoelectronic CO_2 molecule and the valence isolectronic CS_2 molecule. Indeed, the periodic variation of the reaction efficiency seen in Figure 3 for the early and late lanthanides is a manifestation of this requirement as it parallels the variation in promotion energy for both CO_2 and N_2O, but is restricted to fewer elements in the reactions with CO_2. Thus $Gd^+(d^1s^1)$, $La^+(d^2)$, and $Ce^+(d^2)$ exhibit high reactivity in their two non-f valence electron configurations, while the reactions of Pr^+, Nd^+, and Tb^+ with CO_2 are less efficient due to the need to promote an f electron in their ground-state $4f^n5d^06s^1$ configurations to achieve two valence electrons. $Lu^+(6s^2)$ is anomalous in that a 6s rather than a 4f electron would have to

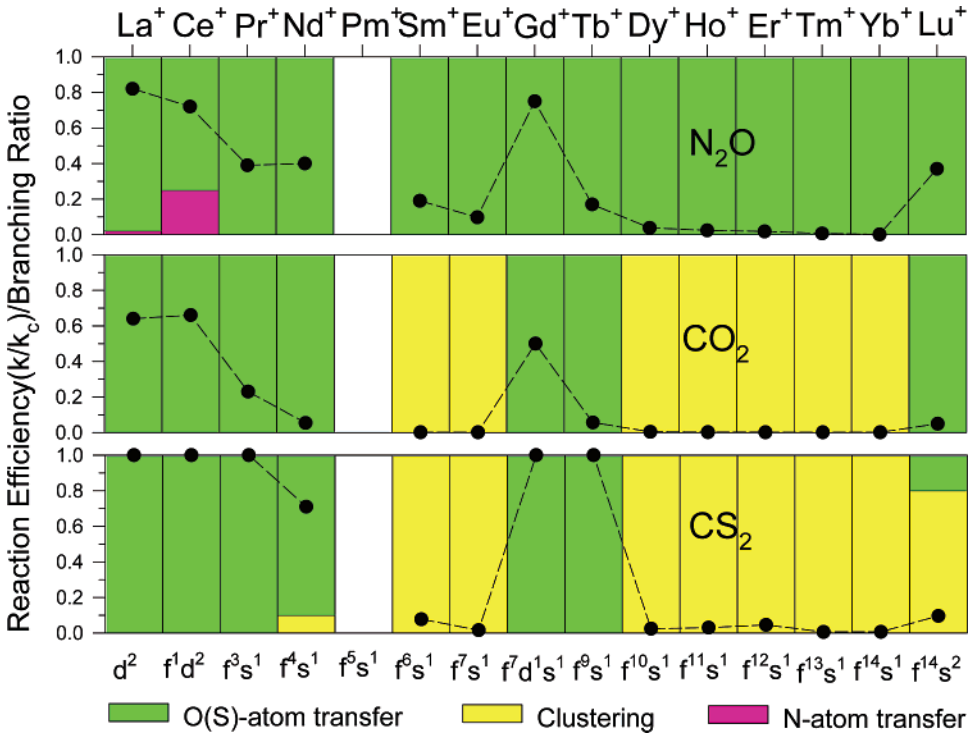

Figure 3. Periodic variations in reaction efficiencies at room temperature for reactions of 14 lanthanide metal cations with CO_2 and CS_2 under ICP/SIFT conditions. Reaction efficiencies (k/k_c) are represented by solid circles. Reaction channels are color coded, and branching ratios are indicated by vertical bars. Previously published results[9] with N_2O are included for comparison.

TABLE 3: Summary of Available Oxygen and Sulfur Atom Affinities (in Units of kcal mol^{-1}) and Various Electronic Properties for Lanthanide Cations

Ln^+	$OA(Ln^+)$[a]	$SA(Ln^+)$	Ln^+ ground-state configuration	Ln^+ term symbol	promotion energy[c] to $5d^16s^1$
La^+	206.6 ± 4.3	124.4 ± 2.4[b]	$5d^2$	$^3F_2$	4.5 ± 3.0
Ce^+	203.6 ± 5.9	125 ± 14[a]	$4f^15d^2$	$^4H_{7/2}°$	4.6 ± 5.7
Pr^+	189.6 ± 4.3		$4f^36s^1$	$(9/2,1/2)_4°$	22.3 ± 0.8
Nd^+	180.8 ± 4.3		$4f^46s^1$	$^6I_{7/2}$	34.8 ± 8.3
Pm^+			$4f^56s^1$	$^7H_2°$	
Sm^+	139.6 ± 4.3		$4f^66s^1$	$^8F_{1/2}$	62.1 ± 5.8
Eu^+	93.2 ± 4.3	59 ± 7[a]	$4f^76s^1$	$^9S_4°$	92.8 ± 5.0
Gd^+	180.0 ± 4.3	106.2 ± 13.8[a]	$4f^75d^16s^1$	$^{10}D_{5/2}°$	0
Tb^+	171.0 ± 5.9		$4f^96s^1$	$(15/2,1/2)_8°$	9.3 ± 8.1
Dy^+	143.4 ± 5.9		$4f^{10}6s^1$	$(8,1/2)_{17/2}$	36.0 ± 6.1
Ho^+	141.3 ± 4.3		$4f^{11}6s^1$	$(15/2,1/2)_8°$	37.8 ± 5.4
Er^+	140.3 ± 4.3		$4f^{12}6s^1$	$(6,1/2)_{13/2}$	34.5 ± 3.1
Tm^+	116.6 ± 4.3		$4f^{13}6s^1$	$(7/2,1/2)_4°$	55.5 ± 7.4
Yb^+	88.1 ± 5.9	59.0 ± 0.1[b]	$4f^{14}6s^1$	$^2S_{1/2}$	79.4 ± 4.0
Lu^+	128.0 ± 4.3	107.2 ± 0.1[b]	$4f^{14}6s^2$	$^1S_0$	36.6 ± 3.6

[a] XA (X = O, S) values were taken on the basis of $\Delta H_f°(LnX^+)$, $\Delta H_f°(Ln^+)$, and $\Delta H_f°(X)$, found in ref 31. [b] SA values were taken on the basis of $\Delta H_f°(Ln^+)$ and $\Delta H_f°(S)$ found in ref 31 and IE(LnS) and $D(Ln-S)$ found in ref 32. [c] In kcal mol^{-1}, taken from ref 9. The promotion energy and accompanying error are taken as the mean and standard deviation of the energy difference between all states in the ground-state manifold transitioning to all possible states in the first excited manifold.

be promoted to a 5d orbital to achieve a d^1s^1 configuration. Apparently such a promotion does not occur, as is evident from the higher reactivity of Lu^+ compared to other late lanthanide cations (Dy^+, Ho^+, Er^+) that have similar or lower promotion energies (PEs) but are much less reactive.

Large variations in reactivity also have been reported for gas-phase reactions of neutral lanthanide atoms with CO_2, and the reaction energy barrier was found to correlate with the energy required to promote an electron out of the filled 6s subshell.[26]

In sharp contrast, no correspondence with electron promotion energy is observed for S-atom transfer to lanthanide cations from the valence isolectronic CS_2 molecule. S-atom transfer at room temperature is observed to proceed with unit efficiency, except in the case of the reactions with Nd^+ and Lu^+.

3.4. Role of the Kinetic Barrier to Atom Transfer. The observed reaction efficiencies and their dependence on electron promotion energy and reaction exothermicity can be understood qualitatively in term of the double-minimum potential energy surface sketched in Figure 5. Proceeding from left to right in Figure 5, the potential energy of the ion/molecule reactants initially decreases as they approach each other due to electrostatic interaction. The consequent kinetic energy of relative motion becomes available to surmount the energy required for electron promotion (PE). Thus the reactivity of Ln^+ ions is expected to decrease with increasing electron promotion energy and become immeasurably small once the kinetic barrier (PE) substantially exceeds the initial energy of the reactants. Thus the reactions of Sm^+, Dy^+, Ho^+, and Er^+ with CO_2, for which

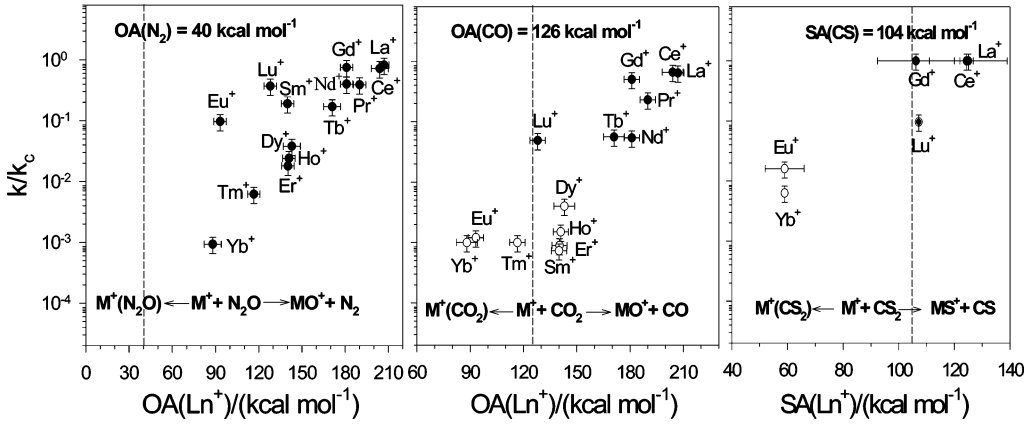

Figure 4. Dependence of reaction efficiency, k/k_c, on O-atom affinity, OA, of Ln^+ for reactions of Ln^+ with N_2O and CO_2, and S-atom affinity, SA, of Ln^+ for reactions of Ln^+ with CS_2. In each panel, reactions on the right of the dashed line are exothermic for atom transfer while those on the left are endothermic. Open circles refer to addition and solid circles to atom abstraction.

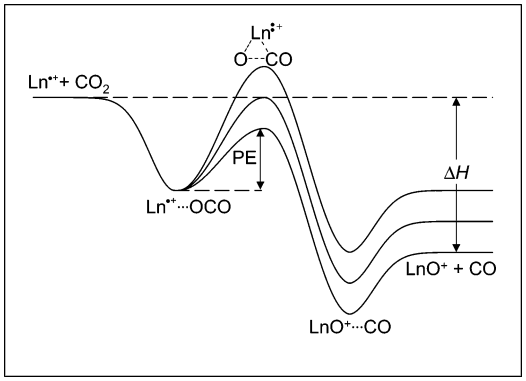

Figure 5. Schematic potential-energy surface for insertion of Ln^+ into a chemical bond (O−CO) for an ion with low (bottom curve), intermediate (middle curve), or high (top curve) $f^n s^1 \rightarrow f^{n-1} d^1 s^1$ promotion energy. (For La^+, Ce^+, and Lu^+, the promotion energy corresponds to the promotion $d^2 \rightarrow d^1 s^1$ or $s^2 \rightarrow d^1 s^1$.)

O-atom transfer is exothermic (see Figure 4), proceed by CO_2 addition because the kinetic barrier (PE) is too high; the promotion energies for the four cations are 62.1, 36.0, 37.8, and 34.5 kcal mol^{-1}, respectively. However, for a family of similar oxidation reactions, the barrier is "dragged down" as the exothermicity (ΔH) increases, viz. OA(Ln^+) increases. Since $\Delta H = OA(X) - OA(Ln^+)$, we can express the physicochemical potential of the Ln^+ to be oxidized, or the oxophilicity Ox-(Ln^+), as PE − OA(Ln^+); see Figure 6. Our measurements indicate that when $Ox(Ln^+) \geq -107$ kcal mol^{-1}, oxidation of Ln^+ with CO_2 becomes kinetically unfavorable.

Figure 4 suggests that a kinetic barrier that decreases with increasing exothermicity operates for O-atom transfer from CO_2 and N_2O, but not for S-atom transfer from CS_2. Why are the latter reactions so special? We note that the strength of the electrostatic attraction due to ion−induced dipole interaction is greater with CS_2 than with CO_2, $\alpha(CS_2) = 8.74$ Å^3 > $\alpha(CO_2) = 2.91$ Å^3, and with N_2O ($\alpha = 3.03$ Å^3, $\mu_D = 0.167$ D).[30] This translates into an increased availability of chemical activation energy (an enhanced well depth for Ln^+-CS_2) in the reactions with CS_2 which is likely to account for the higher efficiency of S compared to O transfer that is observed. Indeed, the observed unit efficiency for S-atom abstraction implies that any kinetic barriers to S-atom transfer (PE in Figure 5) lie below the initial energy of the reactants.

An alternative explanation (offered by one of the reviewers) becomes apparent from a comparison of the CO_2 results with results previously reported for the isoelectronic N_2O molecule. The first observation of a kinetic barrier to reactions of metal ions with N_2O pointed out that the potential energy surface for removing an oxygen atom from N_2O follows a singlet surface to yield $N_2 + O(^1D)$.[33] Thus there is a crossing between the singlet and triplet surfaces of the N_2O, and by analogy CO_2, molecule. The singlet−triplet splitting for O is 1.958 eV, whereas it is only 1.121 eV for S.[34] Because the singlet−triplet splitting is smaller for the sulfur species, the coupling between these two surfaces is energetically more accessible and this could account for the relatively higher reactivity of CS_2.

3.5. CX_2 Addition Reactions. Primary CX_2 addition, reaction 1b, was observed exclusively with Sm^+, Eu^+, Dy^+, Ho^+, Er^+, Tm^+, and Yb^+ with measured reaction rate coefficients in the range from 5.0×10^{-13} (Sm^+) to 2.7×10^{-10} (Dy^+) cm^3 $molecule^{-1}$ s^{-1}. CS_2 addition also was observed exclusively with the same atomic ions with reaction rate coefficients in the range from 5.3×10^{-12} (Tm^+) to 7.4×10^{-11} (Sm^+) cm^3 $molecule^{-1}$ s^{-1}, but also competed with S-atom transfer in the reactions with Nd^+ and Lu^+. The CS_2 addition reactions are about 10 times faster than the CO_2 addition reactions.

Almost all of the primary $Ln^+(CX_2)$ cations added CX_2 according to reaction 2 as did the primary LnX^+ cations

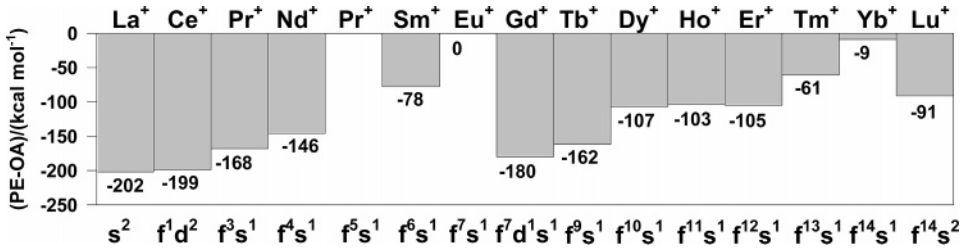

Figure 6. Bar graph showing the variation in PE − OA across the row of the Ln^+ family of cations. PE is the promotion energy required to achieve a d^1s^1 valence configuration, and OA is the O-atom affinity of Ln^+. PE − OA is viewed as a physicochemical potential for the oxidation of Ln^+ cations, $Ox(Ln^+)$ (see text).

according to reaction 3.

$$Ln^+(CX_2)_n + CX_2 \rightarrow Ln^+(CX_2)_{n+1} \quad (2)$$

$$LnX^+(CX_2)_n + CX_2 \rightarrow LnX^+(CX_2)_{n+1} \quad (3)$$

Thus, secondary and higher order CO_2 addition was observed for $Ln^+ = Sm^+$ ($n = 1, 2$) and Eu^+ ($n = 1$) according to reaction 2 and for $LnO^+ = LaO^+$, CeO^+, PrO^+ ($n = 0$), GdO^+ ($n = 0$, 1), TbO^+ ($n = 0-3$), and LuO^+ ($n = 0-4$) according to reaction 3. Secondary and higher order CS_2 addition was observed for $Ln^+ = Nd^+$, Eu^+, Dy^+, Ho^+, Lu^+ ($n = 1-3$), Sm^+, Tm^+, Yb^+ ($n = 1, 2$), and Er^+ ($n = 1-4$) according to reaction 2 and for $LnS^+ = LaS^+$, NdS^+ ($n = 0-2$), CeS^+, PrS^+, GdS^+, and TbS^+ ($n = 0-3$) according to reaction 3. All these addition reactions are expected to proceed in a termolecular fashion with He buffer gas atoms acting as the stabilizing third body.

4. Conclusions

Reactions of atomic lanthanide cations with carbon dioxide and carbon disulfide in the gas phase at room temperature in a helium bath at 0.35 Torr proceed by atom transfer or molecule addition. The kinetics of atom transfer exhibit a periodicity in reaction efficiency and, for O-atom transfer from CO_2, a barrier to reaction that involves the energy required to make available two non-f valence electrons for O-atom bonding (similar to that previously observed with the isoelectronic N_2O molecule). No such barrier is operative for S-atom transfer from the valence isoelectronic CS_2 molecule in which the strong initial electrostatic interaction between the reagents appears to be sufficient to overcome any intrinsic activation barrier that may be present. Secondary atom transfer does not occur. Molecule addition prevails in the absence of atom transfer and in the further reactions of the ionic products of atom transfer. Up to four molecules were observed to add sequentially to selected atomic cations and five to lanthanum oxide or sulfide cations.

Acknowledgment. Continued financial support from the Natural Sciences and Engineering Research Council of Canada is greatly appreciated. Also, we acknowledge support from the National Research Council, the Natural Science and Engineering Research Council, and MDS SCIEX in the form of a Research Partnership grant. As holder of a Canada Research Chair in Physical Chemistry, D.K.B. thanks the Canada Research Chair Program for contributions to this research.

References and Notes

(1) Schilling, J. B.; Beauchamp, J. L. *J. Am. Chem. Soc.* **1988**, *110*, 15.
(2) Azzaro, M.; Breton, S.; Decouzon, M.; Geribaldi, S. *Int. J. Mass Spectrom. Ion Processes* **1993**, *128*, 1.
(3) Cornehl, H. H.; Heinemann, C.; Schroeder, D.; Schwarz, H. *Organometallics* **1995**, *14*, 992.
(4) Carretas, J. M.; Marcalo, J.; Pires de Matos, A. *Int. J. Mass Spectrom.* **2004**, *234*, 51.
(5) Zhao, X.; Koyanagi, G. K.; Bohme, D. K. *Can. J. Chem.* **2005**, *83*, 1839.
(6) Huang, Y.; Wise, M. B.; Jacobson, D. B.; Freiser, B. S. *Organometallics* **1987**, *6*, 346.
(7) Sunderlin, L. S.; Armentrout, P. B. *Int. J. Mass Spectrom. Ion Processes* **1989**, *94*, 149.
(8) Elkind, J. L.; Sunderlin, L. S.; Armentrout, P. B. *J. Phys. Chem.* **1989**, *93*, 3151.
(9) Koyanagi, G. K.; Bohme, D. K. *J. Phys. Chem. A* **2001**, *105*, 8964.
(10) Cheng, P.; Koyanagi, G. K.; Bohme, D. K. *ChemPhysChem* **2006**, *7*, 1813.
(11) Gibson, J. K. *J. Phys. Chem.* **1996**, *100*, 15688.
(12) Geribaldi, S.; Breton, S.; Decouzon, M.; Azzaro, M. *J. Am. Soc. Mass Spectrom.* **1996**, *7*, 1151.
(13) Gibson, J. K.; Haire, R. G. *Radiochim. Acta* **2001**, *89*, 709.
(14) Yin, W. W.; Marshall, A. G.; Marcalo, J.; Pires de Matos, A. N. *J. Am. Chem. Soc.* **1994**, *116*, 8666.
(15) Carretas, J. M.; De Matos, A. P.; Marcalo, J. *Adv. Mass Spectrom.* **1998**, *14*, F037680/1.
(16) Marchande, N.; Breton, S.; Geribaldi, S.; Carretas, J. M.; De Matos, A. P.; Marcalo, J. *Int. J. Mass Spectrom.* **2000**, *195/196*, 139.
(17) Vieira, M. D.; Marcalo, J.; de Matos, A. P. *J. Organomet. Chem.* **2001**, *632*, 126.
(18) Koyanagi, G. K.; Zhao, X.; Blagojevic, V.; Jarvis, M. J. Y.; Bohme, D. K. *Int. J. Mass Spectrom.* **2005**, *241*, 189.
(19) Gibson, J. K. *J. Phys. Chem. A* **2003**, *107*, 7891.
(20) Rue, C.; Armentrout, P. B.; Kretzschmar, I.; Schroder, D.; Harvey, J. N.; Schwarz, H. *J. Chem. Phys.* **1999**, *110*, 7858.
(21) Kretzschmar, I.; Schroeder, D.; Schwarz, H.; Rue, C.; Armentrout, P. B. *J. Phys. Chem. A* **2000**, *104*, 5046.
(22) Rue, C.; Armentrout, P. B.; Kretzschmar, I.; Schroder, D.; Schwarz, H. *Int. J. Mass Spectrom.* **2001**, *210/211*, 283.
(23) Sodupe, M.; Branchadell, V.; Rosi, M.; Bauschlicher, C. W., Jr. *J. Phys. Chem. A* **1997**, *101*, 7854.
(24) Koyanagi, G. K.; Bohme, D. K. *J. Phys. Chem. A* **2006**, *110*, 1232.
(25) Cheng, P.; Koyanagi, G. K.; Bohme, D. K. *J. Phys. Chem. A* **2006**, *110*, 2718.
(26) Campbell, M. L. *Phys. Chem. Chem. Phys.* **1999**, *1*, 3731.
(27) Koyanagi, G. K.; Baranov, V. I.; Tanner, S. D.; Bohme, D. K. *J. Anal. At. Spectrom.* **2000**, *15*, 1207.
(28) Koyanagi, G. K.; Lavrov, V. V.; Baranov, V.; Bandura, D.; Tanner, S.; McLaren, J. W.; Bohme, D. K. *Int. J. Mass Spectrom.* **2000**, *194*, L1.
(29) Su, T.; Chesnavich, W. J. *J. Chem. Phys.* **1982**, *76*, 5183.
(30) Lide, D. R. *CRC Handbook of Chemistry and Physics*, 82nd ed.; CRC Press: Boca Raton, FL, 2001.
(31) Lias, S. G.; Bartmess, J. E.; Liebman, J. F.; Holmes, J. L.; Levin, R. D.; Mallard, W. G. *J. Phys. Chem. Ref. Data* **1988**, Suppl. 17, 861 pp.
(32) Luo, Y.; Wan, X.; Ito, Y.; Takami, S.; Kubo, M.; Miyamoto, A. *Chem. Phys.* **2002**, *282*, 197.
(33) Armentrout, P. B.; Halle, L. F.; Beauchamp, J. L. *J. Chem. Phys.* **1982**, *76*, 2449.
(34) Moore, C. E. *Atomic energy levels as derived from the analyses of optical spectra*; U.S. National Bureau of Standards: Washington, DC, 1971.